Multi-Temporal, Multi-Modal UAV and Machine Learning Framework for Early Detection and Mapping of Bacterial Leaf Blight in Rice

Megharani Doddamani[1], Ziyi Wang[1], Florian J. Ellsäßer[1], Nancy Castilla[2], Alice Laborte[2], Andrew Nelson[1], Stephen Klassen[2], Roshanak Darvishzadeh[1]

[1]Faculty of Geo-information Science and Earth Observation (ITC), University of Twente, Enschede, Netherlands - m.p.doddamani@student.utwente.nl, z.wang-3@utwente.nl, f.j.ellsaesser@utwente.nl, a.nelson@utwente.nl, r.darvish@utwente.nl

[2] International Rice Research Institute (IRRI), Los Banos, Laguna, Philippines - n.castilla@cgiar.org, a.g.laborte@cgiar.org, stephen.p.klassen@gmail.com

KEYWORDS: Bacteria Leaf Blight, UAV, RGB, Multispectral, Thermal, Precision Agriculture

ABSTRACT:

Bacterial leaf blight (BLB), caused by infections with *Xanthomonas oryzae pv. Oryzae* (*Xoo*) bacteria, is one of the most destructive diseases affecting rice cultivation across the globe, frequently leading to severe yield losses. Early detection and timely management before visible symptoms appear and irreversible damage occurs are crucial to mitigating its impact on rice productivity and ensuring food security. Traditional monitoring methods based on field inspections require expert knowledge, are limited to visible symptom stages, and are time-consuming. Recent advancements in remote sensing, particularly with uncrewed aerial vehicles (UAVs), offer new opportunities for timely, quantitative, high-resolution monitoring of crop conditions. This study aimed to develop a multi-temporal, multi-modal UAV-based framework integrating multispectral, thermal, and RGB data to detect and map early-stage BLB infections in rice canopies. During the 2023 wet season at the Zeigler Experiment Station of the International Rice Research Institute (IRRI), an experiment was established using two rice fields, each equally divided into healthy and artificially inoculated plots. Disease severity percentage at specific growth stages, with weekly UAV imagery, were collected throughout the growing season. UAV imagery was processed to derive spectral, thermal, and textural features, including GNDVI, NDRE, canopy temperature, and texture indices. A Random Forest machine learning algorithm was applied to identify the most sensitive indicators of early BLB infection. Our results showed that integrating spectral and thermal features enabled earlier-stage BLB detection. The study offers a deployable, data-driven framework for precision rice disease monitoring, enabling timely intervention and sustainable crop protection strategies.

1. INTRODUCTION

Rice, being the staple food for more than half of the global population, positions its production at the nexus of global food security concerns (Sahasranamam et al., 2023). However, climate change intensifies biotic and abiotic stressors that threaten rice production, including pests, pathogens, and extreme weather events(Wang et al., 2026). Among these, Bacterial leaf blight (BLB), caused by *Xanthomonas oryzae* pv. *oryzae*, is one of the most destructive rice diseases, capable of causing yield reduction ranging from 20% to 80% depending on cultivar susceptibility, infection stage, and environmental conditions (Ashwini et al., 2023; Conde et al., 2025; Rezvi et al., 2023).

BLB epidemics occur when the pathogen is present in the agroecosystem and environmental or management conditions favor its multiplication and spread. Warm temperatures (≈25–34 °C), prolonged rainfall, and high levels of humidity create favorable conditions for infection, while infected seeds, crop residues, and excessive nitrogen fertilization can increase host susceptibility and support pathogen persistence (Sakthivel et al., 2001). Once infection begins, bacterial ingress typically occurs through hydathodes, stomata, or epidermal wounds, followed by proliferation within the xylem tissue, disrupting water transport mechanisms and damaging plant growth (Ashwini et al., 2023).

Early detection of asymptomatic to low infection levels during the early growing stage is crucial for effective management interventions and preventing further pathogen spread (Zhao et al., 2024). Traditional on-site scouting remains the predominant monitoring approach; however, it is labor-intensive, requires expert knowledge, remains qualitative, and is often limited to detecting advanced disease stages (Mukherjee et al., 2019). Satellite-based monitoring has also been explored (Yuan et al., 2017), but its relatively coarse spatial resolution limits its usefulness for field-level management. In addition, BLB outbreaks often occur during prolonged rainy and cloudy periods, when optical satellite imagery is frequently unavailable (Yudarwati et al., 2020).

In contrast, uncrewed aerial systems (UAS) provide high-resolution (<2 cm) and repeatable observations of rice canopies from flexible viewing angles. Their ability to carry multiple sensors enables the detection of subtle physiological and structural changes before visible symptom expression, providing a powerful complement to traditional scouting and satellite

https://doi.org/10.5194/isprs-archives-XLIX-B3-2026-1451-2026 |

monitoring (Zhou et al., 2021). Consequently, UAV-based remote sensing has rapidly expanded for BLB detection, using spectral, thermal, textural, and temporal information to identify disease progression (Wijayanto et al., 2024).

Despite these advances, early-stage detection of BLB in rice remains limited. Most existing approaches focus on symptomatic or later growth stages and often rely on spectral indices alone, rarely integrating multi-modal or multi-temporal UAV data. This leaves the critical pre-visual stage largely unmonitored, when disease management would be most effective.

The main objective of this study is to identify the most sensitive spectral, thermal, and textural features derived from multi-temporal and multi-modal UAV data for detecting early BLB incidence. Based on this analysis, a machine learning workflow using Random Forest is developed and validated to enable early detection and mapping of BLB using both RGB imagery alone and the full set of spectral features derived from UAV data.

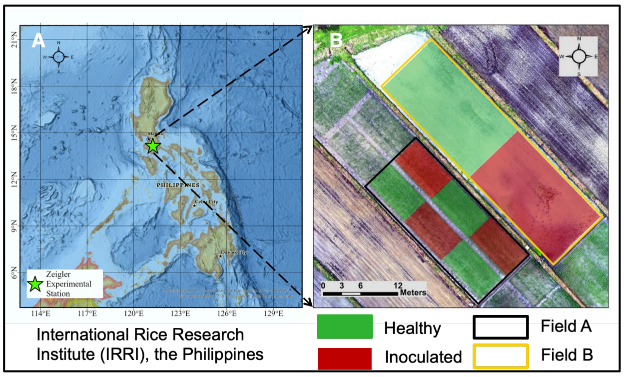

Figure 1: Study area and experimental design (Source: {Citation}

2. MATERIALS AND METHODS

2.1 Study area

The study was conducted at the International Rice Research Institute (IRRI) located in Los Baños, Laguna, Philippines (121°15′ E, 14°10′ N) *(Figure 1).* The region has a tropical climate with distinct wet and dry seasons, providing suitable conditions for rice cultivation. The experiment was carried out during the 2023 wet season at the Zeigler Experiment Station. Two experimental fields (Field A and Field B) were used for the study, where a disease-susceptible rice variety (IR 24) was cultivated. Field A was transplanted on 25 July 2023 and inoculated on 14 August 2023, while Field B was transplanted on 25 August 2023 and inoculated on 5 September 2023.

2.2 Field data

Field data were collected during the 2023 wet season to quantify BLB infection levels and crop conditions. UAV flights were conducted on multiple dates between 10 August and 8 November, covering several rice growth stages including tillering, booting/heading, flowering, soft dough, hard dough, and maturity. Ground truth data were collected during three observation periods corresponding to the stem elongation (SE) and booting (BT) stages at the leaf level from square plots (0.5 × 0.5 m) distributed across the experimental fields and later aggregated to the plot level for model validation. For early disease detection, observations within 0–17 days after inoculation (DAI) were defined as the early stage, representing asymptomatic to low infection conditions.

2.3 Platform and sensor

The UAV flights were carried out by the International Rice Research Institute (IRRI) using a DJI Inspire 2 equipped with a MicaSense Altum multispectral camera, which captures five spectral bands (red, green, blue, NIR, and red-edge) and a thermal band. In addition, RGB imagery was acquired using a DJI Mavic 2 Pro UAV with an integrated camera. The missions were flown at an altitude of 25–30 m above ground level with an image overlap of 75% to the front and side, and GPS positioning was used during data acquisition. Ground control points (GCPs) were placed and measured to improve georeferencing accuracy. Flights were conducted between 08:00 and 11:00 AM under stable weather conditions to ensure consistent illumination. The resulting ground sampling distance (GSD) was approximately 0.6 cm for RGB imagery, 1.2 cm for multispectral imagery, and 18.98 cm for thermal imagery.

3. METHODOLOGY

3.1 Data Pre-processing

The UAV images were processed using Pix4D mapper software to generate orthomosaics and surface models. The images were first aligned and calibrated using the camera’s internal parameters, followed by bundle block adjustment to optimize camera positions. GCPs were used to improve the georeferencing accuracy of the dataset. A dense point cloud, digital surface model (DSM), and orthomosaic were then generated from the aligned images.

3.2 Feature extraction and selection

In total, 33 features were considered in this study, including spectral, thermal, and textural features. Among these, 24 were textural features derived from RGB imagery using grey-level co-occurrence matrix (GLCM) analysis, these included eight Haralick texture metrics (energy, entropy, correlation, homogeneity, contrast, cluster shade, cluster prominence, and Haralick correlation) computed across the three RGB bands. In addition, spectral and thermal features such as RGB, NIR, Red-edge, NDRE, GNDVI, CWSI, and TVDI were also evaluated.

Since the imagery was acquired using two UAV sensors, all datasets were first co-registered to ensure spatial alignment between RGB, multispectral, and thermal imagery. Prior to feature extraction, soil pixels were removed using a vegetation mask, where NDVI > 0.2 was applied as the primary threshold. For dates where NDVI was unavailable, an Excess Green (ExG) index combined with Otsu thresholding was used to separate vegetation from soil, ensuring that all extracted features represented canopy characteristics rather than background soil.

To integrate UAV-derived variables with field observations, zonal statistics were applied to extract pixel values of texture features, spectral bands, vegetation indices (VIs), and thermal variables within each experimental plot polygon. For each UAV acquisition date, raster datasets were clipped using the plot boundaries, and pixel values within each plot were analyzed. The mean value of all valid pixels within each plot was used to represent the feature value for that plot. These extracted features were subsequently merged with field-measured BLB severity data using the corresponding plot code and observation date.

To identify the most relevant texture indicators for BLB detection, feature selection was performed using Pearson correlation analysis between each texture feature and field-measured BLB severity. Features showing statistically significant relationships ($p < 0.1$) were retained. From these, the texture features with the strongest positive and strongest negative correlations with BLB were selected as representative indicators. These two selected texture features were then combined to construct a Normalized Difference Texture Index (NDTI).

3.3 Machine Learning Modeling and Model Comparison

To evaluate the capability of UAV-derived features for BLB detection, a Random Forest (RF) model was employed, given its robustness and ability to capture complex non-linear relationships between UAV-derived features and BLB severity. The extracted features were combined with field-measured BLB severity data and used as predictor variables. Model performance was evaluated using cross-validation to ensure robustness while hyperparameter optimization was performed using a randomized search approach to identify the optimal model configuration. Feature importance was further analyzed using SHapley Additive exPlanations (SHAP) to identify the most influential features contributing to BLB detection.

Two modeling scenarios were tested. The first used RGB-only, while the second combined RGB, texture features, with spectral and thermal variables (NIR, Red-edge, NDRE, GNDVI, CWSI, and TVDI). Model performance was assessed using overall accuracy (OA), kappa coefficient, and RMSE to compare RGB-only and multi-modal approaches.

3.4 Early BLB Likelihood Mapping

Early BLB likelihood maps were generated using the probability outputs of the Random Forest model. For each UAV acquisition date, plot-level predictions were obtained by averaging pixel-wise model probabilities within each plot polygon. To improve robustness, the mean probability across three early observation dates (0–17 days after inoculation) was computed to represent early-stage BLB likelihood. The resulting continuous probability values (0–1) were further classified into five likelihood levels (very low, low, moderate, high, and very high) using equal interval thresholds (0–0.2, 0.2–0.4, 0.4–0.6, 0.6–0.8, and 0.8–1.0) for visualization and interpretation.

4. RESULTS AND DISCUSSION

4.1 Texture Feature Correlation Analysis

Pearson correlation analysis revealed distinct relationships between Haralick texture features and BLB severity *(Figure 2)*. Blue_Contrast and Blue_Correlation exhibited the strongest positive and negative correlations, respectively, indicating their high sensitivity to canopy structural changes associated with early disease development.

Based on these findings, the Normalized Difference Texture Index (NDTI) was constructed using the most informative texture features, enabling improved representation of early-stage infection patterns.

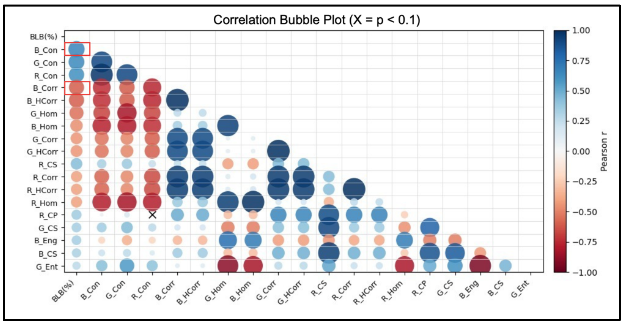

Figure 2: Pearson correlation of Haralick texture features with BLB severity. Blue = positive and red = negative correlations; circle size indicates strength. Crossed cells show non-significant correlations (p > 0.1). Blue_Contrast and Blue_Correlation show the strongest correlations used for NDTI.

4.2 Model Performance Comparison

The selected full spectrum model outperformed the RGB-only model, indicating that integrating spectral, thermal, and texture features improved early BLB detection. From the repeated grouped evaluation, the RGB-only model achieved an accuracy of 0.640, a kappa coefficient of 0.27, RMSE of 0.59, F1 score of 0.62 and ROC-AUC of 0.703, whereas the selected full spectrum model achieved an accuracy of 0.768, kappa coefficient of 0.53, RMSE of 0.47, F1 score of 0.76 and ROC-AUC of 0.845.

As shown in *Figure 3*, the confusion matrices further illustrate the improved classification performance of the selected full spectrum model compared to the RGB-only model. These results demonstrate that combining RGB features with additional spectral, thermal, and texture-based variables enhanced the model's ability to detect BLB-related canopy changes. The improvement was consistent across repeated grouped splits.

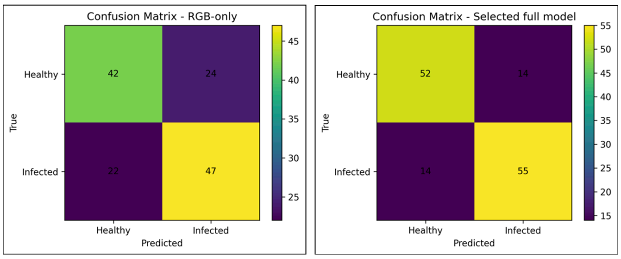

Figure 3: Confusion matrix comparing the performance of the RGB-only Random Forest model and the selected full spectrum model

4.3 Temporal Generalization

The models trained on early-stage data (0–17 DAI) were evaluated on later observation dates to assess their temporal generalization capability. The RGB-only model achieved an accuracy of 0.674, a kappa coefficient of 0.34, and an RMSE of 0.57, while the selected full spectrum model obtained an accuracy of 0.720, a kappa coefficient of 0.44, and an RMSE of 0.52 (Figure 4).

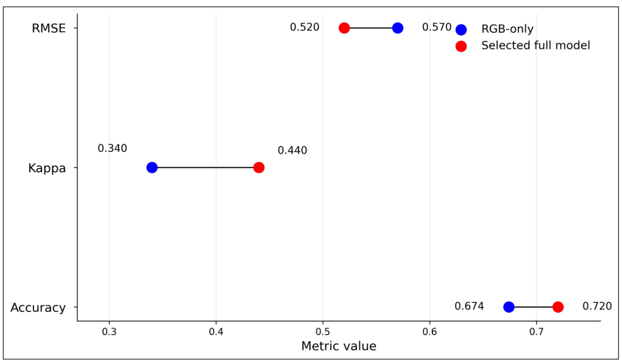

Figure 4: Connected dot plot comparing the performance of the RGB-only baseline and the selected full spectrum model

These results indicate that the full spectrum model maintained consistently improved predictive performance across time, suggesting that the integrated feature set remained effective for detecting BLB at later stages of disease progression.

4.4 Feature Importance

Feature importance analysis using SHAP *(Figure 5)* revealed that NDRE(0.073), GNDVI(0.057), R(0.048), NIR(0.045), and Red-edge(0.034) were the most influential predictors. Additional variables contributing to the model included NDTI, G, Blue_Inertia/Contrast, Blue_correlation, B, TVDI, and CWSI.

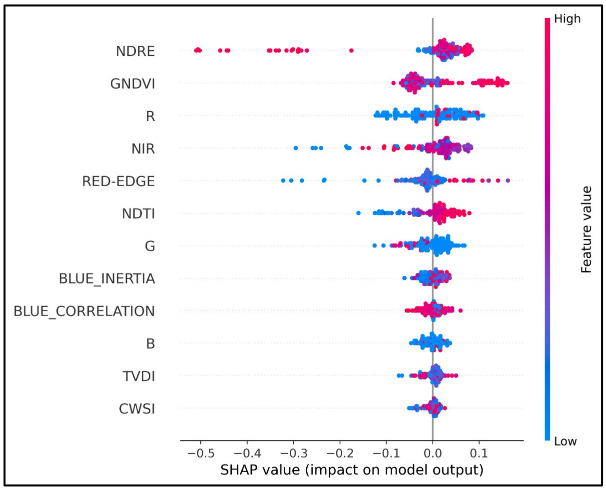

Figure 5: SHAP plot showing feature contributions to the Random Forest model for early BLB detection.

These findings suggest that Red-edge and Near-Infrared sensitive variables played a critical role in BLB detection, as they are strongly related to vegetation physiological stress. Texture-based variables, particularly NDTI, Blue_contrast, and Blue_correlation, also contributed meaningful information, highlighting the importance of canopy structural characteristics in distinguishing healthy and infected rice plots.

4.5 Important findings

The spatial distribution of predicted early BLB likelihood exhibits clear heterogeneity across the experimental fields *(Figure 6),* reflecting distinct patterns of plant physiological response. Areas characterized by high and very high likelihood values are predominantly concentrated within the central and lower plot regions, suggesting the presence of early-stage disease development or increased susceptibility. In contrast, upper plot sections consistently display low likelihood values, indicative of relatively healthy or unaffected vegetation conditions.

A comparative assessment between the RGB-only and full-spectrum models reveals notable differences in spatial coherence and sensitivity. The full spectrum model produces a more spatially consistent and less noisy representation of disease likelihood, indicating an enhanced capability to capture subtle physiological variations associated with early BLB infection. This improvement can be attributed to the integration of multispectral and thermal features, which provide additional information on chlorophyll dynamics, canopy water status, and plant stress responses that are not adequately captured by RGB data alone.

Furthermore, transitional zones between low and high likelihood regions are distinctly observable, delineating potential early infection fronts. These gradient regions are of particular significance, as they may represent potential early infection fronts prior to visible symptom expression.

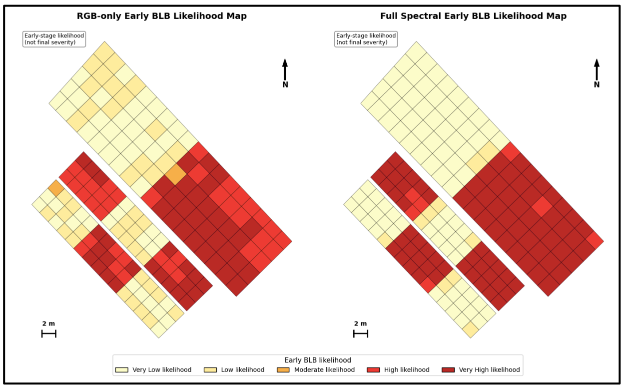

Figure 6: Early BLB likelihood maps from (a) RGB-only and (b) full spectral models, the maps illustrate relative likelihood of early infection, with higher values indicating increased physiological stress.

5 CONCLUSIONS

This study demonstrates that integrating multi-temporal, multimodal UAV data with machine learning enables effective early detection and mapping of BLB in rice canopies. The full spectrum model consistently outperforms the RGB-only approach, underscoring the importance of incorporating spectral, thermal, and textural features for capturing early physiological stress signals.

The ability to identify early-stage infection zones and transition fronts prior to visible symptoms underscores the potential of the proposed framework for precision disease monitoring. These findings support the application of UAV-based multi-modal sensing as a reliable and scalable tool for timely intervention and sustainable crop protection strategies.

ACKNOWLEDGEMENTS

This study was supported by the Netherlands Organisation for Scientific Research (NWO) through the NL-CGIAR Senior Expert grant held by Dr Darvishzadeh.

REFERENCES

Ashwini, S., Prashanthi, S. K., Krishnaraj, P. U., Iliger, K. S., & Kolur, S. M. (2023). Biological Management of Bacterial Leaf Blight of Rice (Xanthomonas oryzae pv. Oryzae) through Rice Rhizosphere Antagonist Actinobacteria. *International Journal of Environment and Climate Change*, *13*(7), 660–673. https://doi.org/10.9734/ijecc/2023/v13i71918

Conde, S., Catarino, S., Ferreira, S., Temudo, M. P., & Monteiro, F. (2025). Rice Pests and Diseases Around the World: Literature-Based Assessment with Emphasis on Africa and Asia. *Agriculture*, *15*(7), 667. https://doi.org/10.3390/agriculture15070667

Mukherjee, A., Misra, S., & Raghuwanshi, N. S. (2019). A survey of unmanned aerial sensing solutions in precision agriculture. *Journal of Network and Computer Applications*, *148*, 102461. https://doi.org/10.1016/j.jnca.2019.102461

Rezvi, H. U. A., Tahjib-Ul-Arif, Md., Azim, Md. A., Tumpa, T. A., Tipu, M. M. H., Najnine, F., Dawood, M. F. A., Skalicky, M., & Brestič, M. (2023). Rice and food security: Climate change implications and the future prospects for nutritional security. *Food and Energy Security*, *12*(1), e430. https://doi.org/10.1002/fes3.430

Sahasranamam, V., Ramesh, T., & Rajeswari, R. (2023). Monitoring and Identifying Paddy Leaf Diseases Using Unmanned Aerial Vehicles (UAVs) with Machine Learning- A Survey. *2023 IEEE 2nd International Conference on Industrial Electronics: Developments & Applications (ICIDeA)*, 560–566. https://doi.org/10.1109/ICIDeA59866.2023.10295173

Sakthivel, N., Mortensen, C. N., & Mathur, S. B. (2001). Detection of Xanthomonas oryzae pv. Oryzae in artificially inoculated and naturally infected rice seeds and plants by molecular techniques. *Applied Microbiology and Biotechnology*, *56*(3–4), 435–441. https://doi.org/10.1007/s002530100641

Wang, Z., Darvishzadeh, R., Laborte, A., Castilla, N., & Nelson, A. (2023). *Understanding the effects of bacterial leaf blight disease on rice spectral signature*. https://doi.org/10.5281/ZENODO.10400333

Wang, Z., Darvishzadeh, R., & Nelson, A. (2026). Remote sensing-based rice stress and health assessment: Current and future perspectives. *International Journal of Remote Sensing*, *47*(4), 1759–1808. https://doi.org/10.1080/01431161.2026.2612851

Wijayanto, A. K., Prasetyo, L. B., Hudjimartsu, S. A., Sigit, G., & Hongo, C. (2024). Textural features for BLB disease damage assessment in paddy fields using drone data and machine learning: Enhancing disease detection accuracy. *Smart Agricultural Technology*, *8*, 100498. https://doi.org/10.1016/j.atech.2024.100498

Yuan, L., Zhang, H., Zhang, Y., Xing, C., & Bao, Z. (2017). Feasibility assessment of multi-spectral satellite sensors in monitoring and discriminating wheat diseases and insects. *Optik*, *131*, 598–608. https://doi.org/10.1016/j.ijleo.2016.11.206

Yudarwati, R., Hongo, C., Sigit, G., Barus, B., & Utoyo, B. (2020). Bacterial Leaf Blight Detection in Rice Crops Using Ground-Based Spectroradiometer Data and Multi-temporal Satellites Images. *Journal of Agricultural Science*, *12*(2), 38. https://doi.org/10.5539/jas.v12n2p38

Zhao, D., Cao, Y., Li, J., Cao, Q., Li, J., Guo, F., Feng, S., & Xu, T. (2024). Early Detection of Rice Leaf Blast Disease Using Unmanned Aerial Vehicle Remote Sensing: A Novel Approach Integrating a New Spectral Vegetation Index and Machine Learning. *Agronomy*, *14*(3), 602. https://doi.org/10.3390/agronomy14030602

Zhou, X.-G., Zhang, D., & Lin, F. (2021). UAV Remote Sensing: An Innovative Tool for Detection and Management of Rice Diseases. In D. Kurouski (Ed.), *Diagnostics of Plant Diseases*. IntechOpen. https://doi.org/10.5772/intechopen.95535